Implicitly extrapolated geometric multigrid on disk-like domains for the gyrokinetic Poisson equation from fusion plasma applications

Martin J. Kühn (DLR/CERFACS)
Carola Kruse (CERFACS) and Ulrich Rüde (FAU/CERFACS)

E·C·E
European Commission
Horizon 2020
European Union funding
for Research & Innovation

DLR

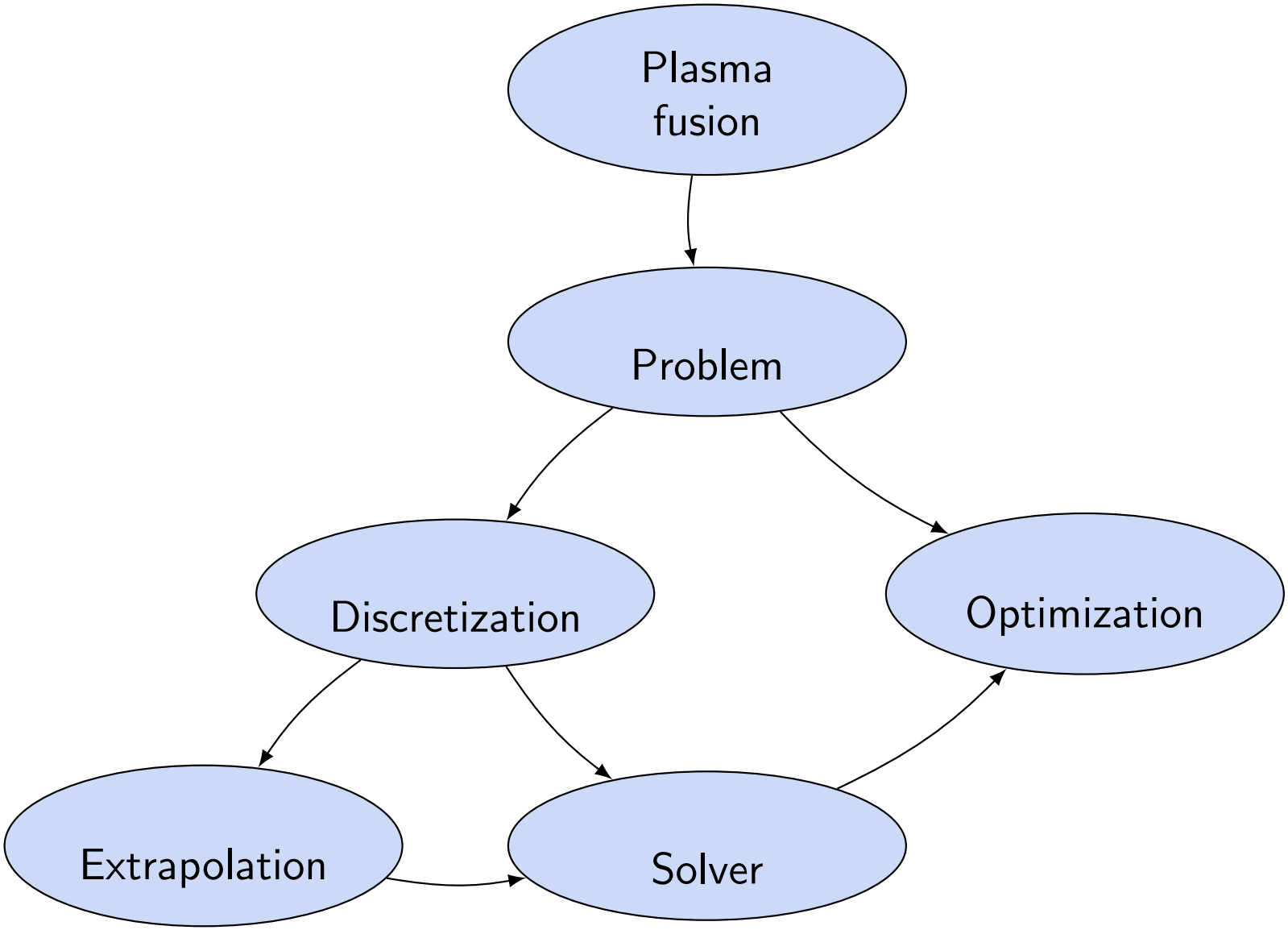
Plasma fusion
Problem
Discretization
Optimization
Extrapolation
Solver

Tokamak geometry and GYSELA solver

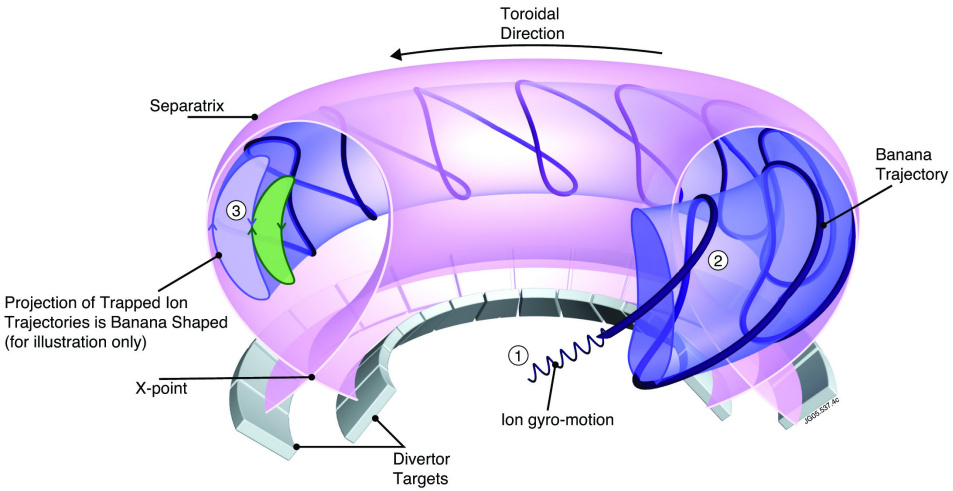

Tokamak schematic picture; from https://www.euro-fusion.org/

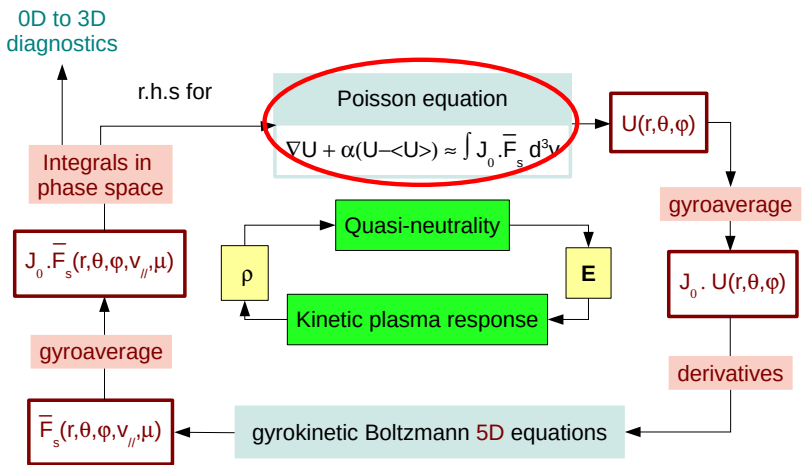

GYSELA schematic picture; courtesy of Virginie Grandgirard

V. Grandgirard, J. Abiteboul, J. Bigot, T. Cartier-Michaud, N. Crouseilles, G. Dif-Pradalier, Ch. Ehrlacher, D. Esteve, X. Garbet, Ph. Ghendrih, G. Latu, M. Mehrenberger, C. Norscini, Ch. Passeron, F. Rozar, Y. Sarazin, E. Sonnendrücker, A. Strugarek, D. Zarzoso, *A 5D gyrokinetic full-f global semi-Lagrangian code for flux-driven ion turbulence simulations* Computer Physics Communications 207 (2016) 35–68

Poloidal cross section and curvilinear coordinates

Disk-like geometry:

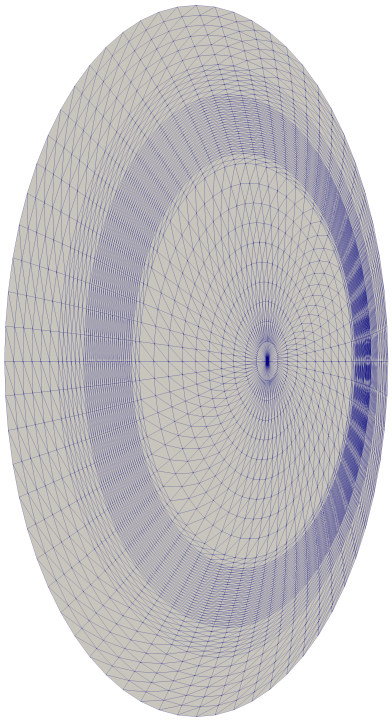

N. Bouzat, C. Bressan, V. Grandgirard, G. Latu, and M. Mehrenberger, *Targeting realistic geometry in tokamak code gysela*, ESAIM: ProcS, 63 (2018), pp. 179–207

Poloidal cross section and curvilinear coordinates

Disk-like geometry:

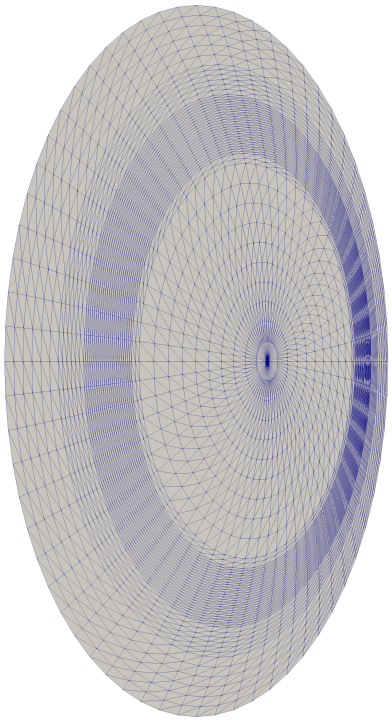

N. Bouzat, C. Bressan, V. Grandgirard, G. Latu, and M. Mehrenberger, *Targeting realistic geometry in tokamak code gysela*, ESAIM: ProcS, 63 (2018), pp. 179–207

Simplified mapping:

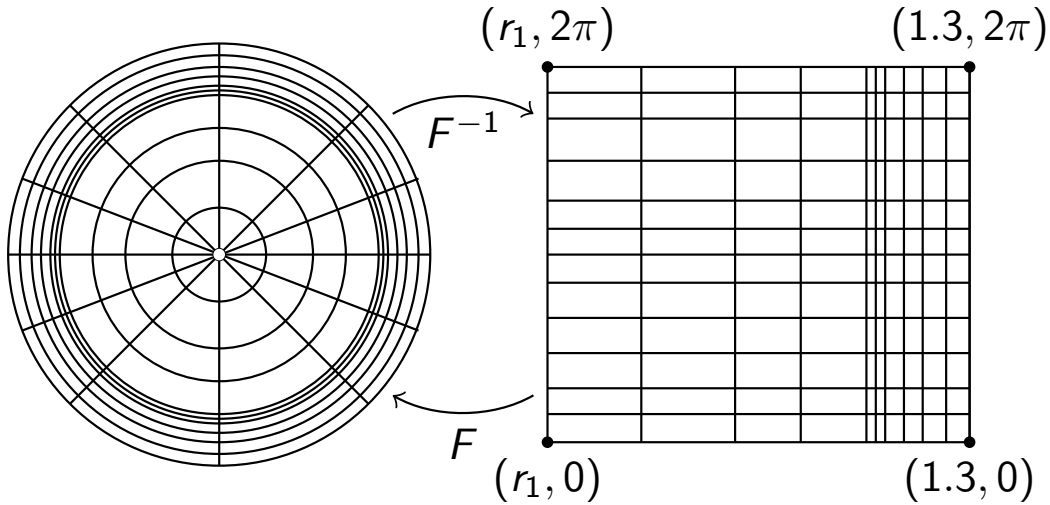

Simplified phyiscal (left) and logical (right) domain for $r_1 > 0$ and polar coordinate transformation with anisotropic tensor-product mesh.

Poloidal cross section and curvilinear coordinates

Disk-like geometry:

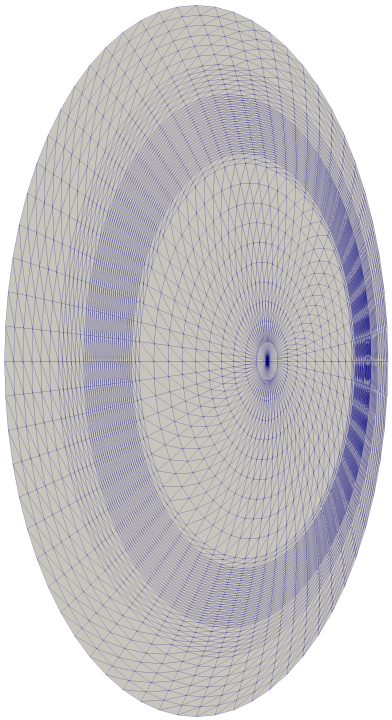

N. Bouzat, C. Bressan, V. Grandgirard, G. Latu, and M. Mehrenberger, *Targeting realistic geometry in tokamak code gysela*, ESAIM: ProcS, 63 (2018), pp. 179–207

Simplified mapping:

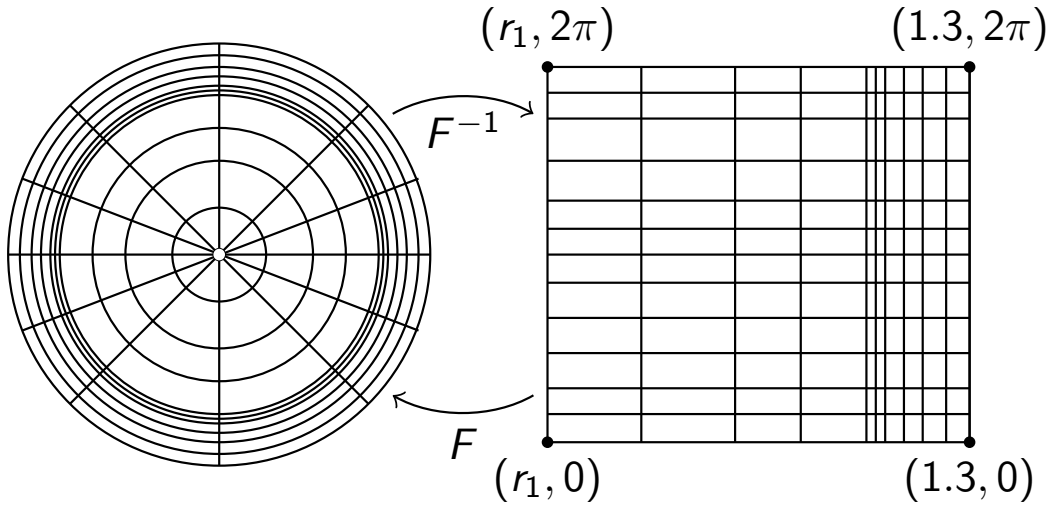

Simplified phyiscal (left) and logical (right) domain for $r_1 > 0$ and polar coordinate transformation with anisotropic tensor-product mesh.

$$x = (1-\kappa) r \cos(\theta) - \delta r^2,$$
$$y = (1+\kappa) r \sin(\theta),$$
$$(r, \theta) \in [r_1, 1.3] \times [0, 2\pi], \kappa = 0.3, \delta = 0.2.$$

Gyrokinetic Poisson equation: Density profile and anisotropic grid

$$
\begin{aligned}
-\nabla \cdot (\alpha \nabla u) &= f \quad \text{in } \Omega \\
u &= 0 \quad \text{on } \partial\Omega
\end{aligned}
$$

- $\Omega \subset \mathbb{R}^2$: poloidal cross section
- f: rhs obtained from half-step before
- α: density profile

$$
\alpha(r) = \frac{2}{2.6 + 3.14} \left(1.3 + \arctan\left(\frac{1 - r}{0.09}\right)\right)
$$

[Eric Sonnendrücker, private communication (2019).]

Gyrokinetic Poisson equation: Density profile and anisotropic grid

$$-\nabla \cdot (\alpha \nabla u) = f \quad \text{in } \Omega$$
$$u = 0 \quad \text{on } \partial\Omega$$

- $\Omega \subset \mathbb{R}^2$: poloidal cross section
- f: rhs obtained from half-step before
- α: density profile

$$\alpha(r) = \frac{2}{2.6 + 3.14}\left(1.3 + \arctan\left(\frac{1-r}{0.09}\right)\right)$$

[Eric Sonnendrücker, private communication (2019).]

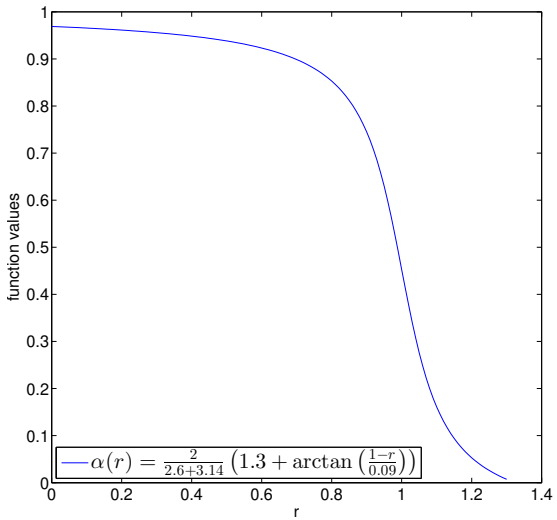

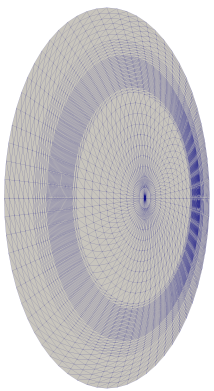

Discretization at or "across" the origin

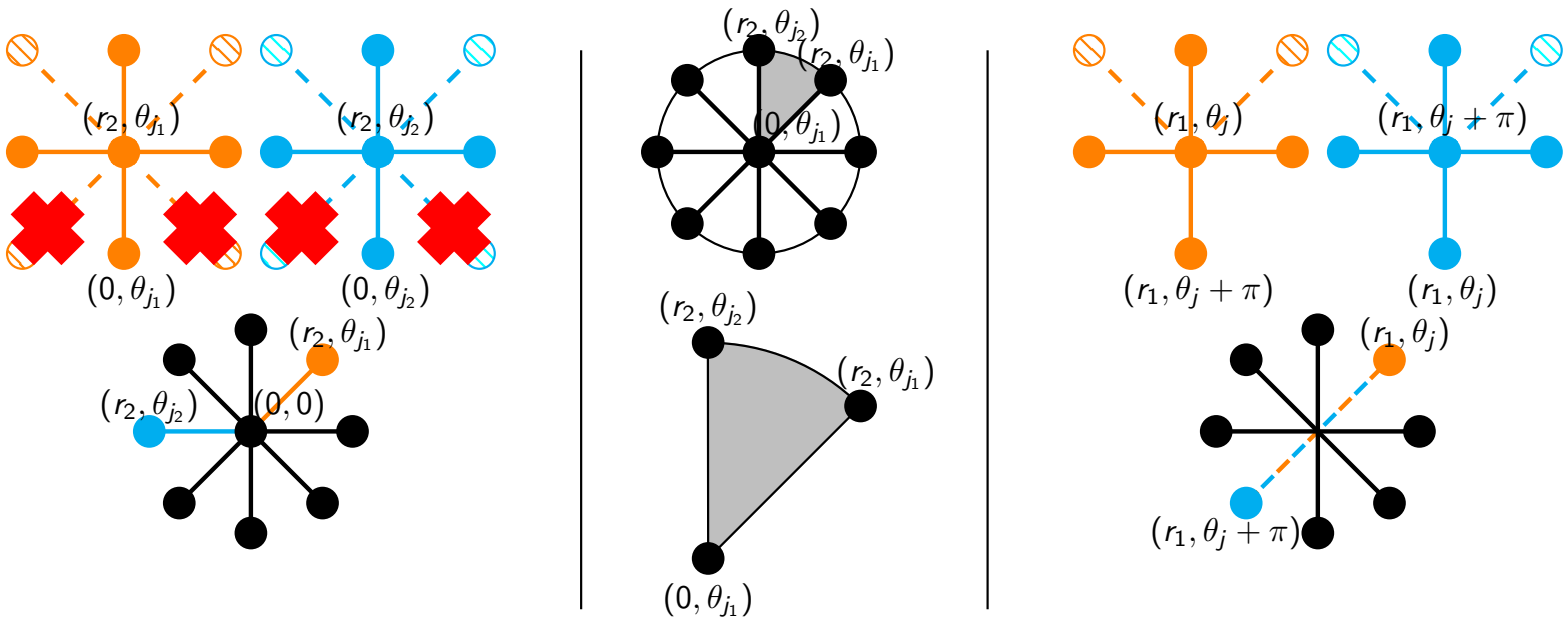

Figure: FD around $r_1 = 0$ (left), FE around $r_1 = 0$ (center), FD/FE across the origin for $r_1 > 0$ (right).

The multigrid cycle

$u_l^{m+1} = \mathbf{MGC}(l, \gamma, u_l^m, K_l, f_l, \nu_1, \nu_2)$

- Presmoothing: $u_l^{m+1/3} = \mathbf{S}^{\nu_1}(u_l^m, K_l, f_l)$
- Coarse grid correction
  - Compute the residual
  - Restrict the residual
  - Solve $A_{l-1}\widehat{e}_{l-1}^{m+2/3} = r_{l-1}^{m+2/3}$ by
    - (if $l = 0$:) the use of a direct solver.
    - (if $l \geq 1$:) γ-times recursively calling $\widehat{e}_{l-1}^{m+2/3} = \mathbf{MGC}(l-1, \gamma, \diamondsuit, K_{l-1}, r_{l-1}^{m+2/3}, \nu_1, \nu_2)$
  - Interpolate the correction
  - Compute the corrected approximation
- Postsmoothing: $u_l^{m+1} = \mathbf{S}^{\nu_2}(u_l^{m+2/3}, K_l, f_l)$

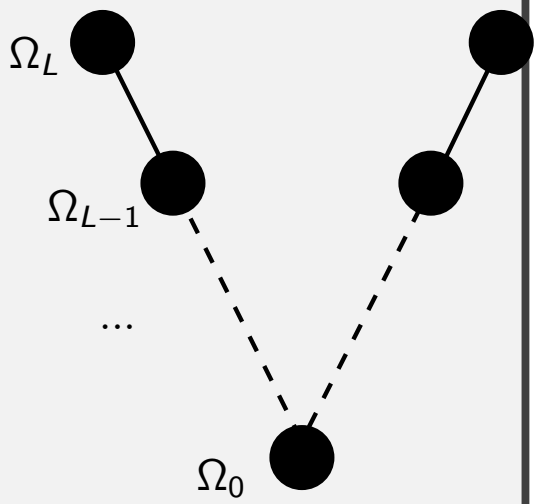

Implicit extrapolation between Ω_L and Ω_{L-1}

- Indices $\cdot_c$ for coarse and $\cdot_f$ for fine nodes:

$$K_L = \begin{pmatrix} K_{L,cc} & K_{L,cf} \\ K_{L,fc} & K_{L,ff} \end{pmatrix}, \quad f_l = \begin{pmatrix} f_{L,c} \\ f_{L,f} \end{pmatrix}, \quad u_l^m = \begin{pmatrix} u_{L,c}^m \\ u_{L,f}^m \end{pmatrix}.$$

- Extrapolated stiffness matrix and vector

$$K_L^{ex} := \begin{pmatrix} \frac{4}{3}K_{L,cc} - \frac{1}{3}K_{L-1} & \frac{4}{3}K_{L,cf} \\ \frac{4}{3}K_{L,fc} & \frac{4}{3}K_{L,ff} \end{pmatrix} \quad \text{and} \quad f_F^{ex} := \begin{pmatrix} \frac{4}{3}f_{L,c} - \frac{1}{3}f_{L-1} \\ \frac{4}{3}f_{L,f} \end{pmatrix}$$

  are equal to those of a quadratic basis (nonstandard FE integration).
- Modified intergrid transfer operator I_L^{L-1} yields new residual

$$\begin{aligned} &\frac{4}{3} I_L^{L-1}\left(f_L - K_L u_L^{m+1/3}\right) - \frac{1}{3}\left(f_{L-1} - K_{L-1} u_{L,c}^{m+1/3}\right) \\ =&I_L^{L-1}\left[f_L^{ex} - K_L^{ex} u_L^{m+1/3}\right]. \end{aligned}$$

The implicitly extrapolated multigrid cycle

$$u_L^{m+1} = \mathbf{IEMGC}(L, \gamma, u_L^m, K_L, f_L, \nu_1, \nu_2)$$

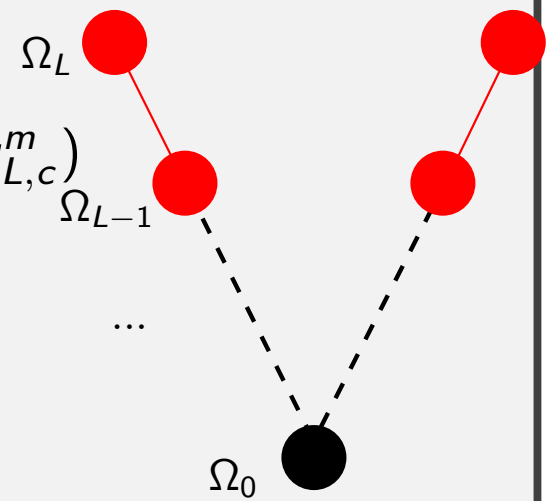

- Presmoothing: $u_{L,f}^{m+1/3} = \mathbf{S}^{\nu_1}(u_{L,f}^m, K_{L,ff}, f_{L,f} - K_{L,fc} u_{L,c}^m)$
- Define iterate: $u_L^{m+1/3} = \begin{pmatrix} u_{L,c}^m \\ u_{L,f}^{m+1/3} \end{pmatrix}$
- Coarse grid correction
  - Compute and restrict the residual:
    $$r_{L-1}^{m+2/3} = \tfrac{4}{3} I_L^{L-1}(f_L - K_L u_L^{m+1/3}) - \tfrac{1}{3}(f_{L-1} - K_{L-1} u_{L,c}^{m+1/3})$$
  - Call a standard multigrid cycle on $L-1$ levels:
    $$\widehat{e}_{L-1}^{m+2/3} = \mathbf{MGC}(L-1, \gamma, 0, K_{L-1}, r_{L-1}^{m+2/3}, \nu_1, \nu_2)$$
  - Interpolate and correct approximation:
    $$u_l^{m+2/3} = u_l^{m+1/3} + I_{L-1}^L \widehat{e}_{L-1}^{m+2/3}$$
- Postsmoothing: $u_{L,f}^{m+1} = \mathbf{S}^{\nu_2}(u_{L,f}^m, K_{L,ff}, f_{L,f} - K_{L,fc} u_{L,c}^{m+2/3})$
- Define iterate: $u_L^{m+1} = \begin{pmatrix} u_{L,c}^{m+2/3} \\ u_{L,f}^{m+1} \end{pmatrix}$

Multigrid smoothing for curvilinear coordinates

- Curvilinear coordinates: e.g. polar coordinates
- Pointwise smoothers are not sufficient
- (Zebra) line smoothers were proposed (Stüben/Trottenberg/Barros)

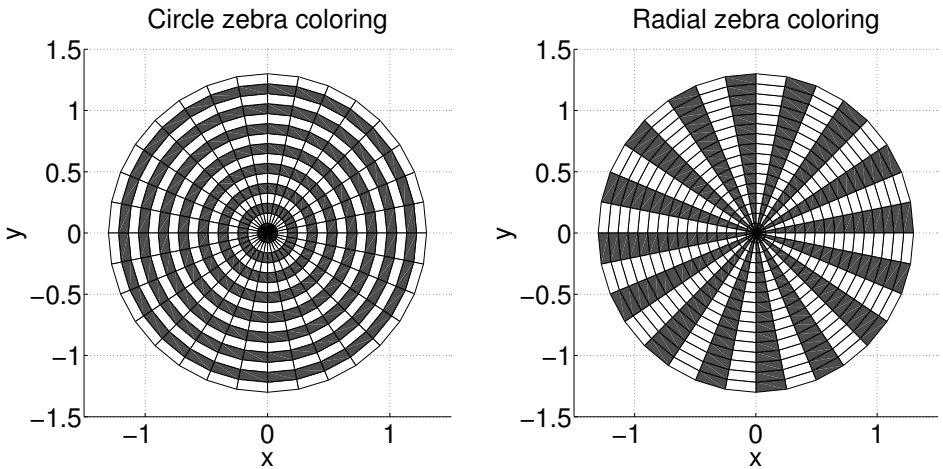

- Curvilinear coordinates lead to changing anisotropy across the grid (e.g., factor $1/r$)
- Use of circle **and** radial smoothers on all nodes, to overcome changing strong connections, nonoptimal in computational efficiency

Circle and radial smoothing factors on annulus $(r_i, r_i + h_i) \times [0, 2\pi)$

$$\mu_{\mathrm{CZ},h_i,k_j} = \max_{r_i \le r \le r_i + h_i} \left\{ \left(\frac{q_{i,j}^2 r^2}{1 + q_{i,j}^2 r^2} \right)^2, C_C \right\}; C_C \in \{0.23, 0.34\}$$

$$\mu_{\mathrm{RZ},h_i,k_j} = \max_{r_i \le r \le r_i + h_i} \left\{ \left(\frac{1}{1 + q_{i,j}^2 r^2} \right)^2, C_R \right\}; C_R = 0.23$$

with $q_{i,j} = \frac{k_j}{h_i}$; see Barros (1988).

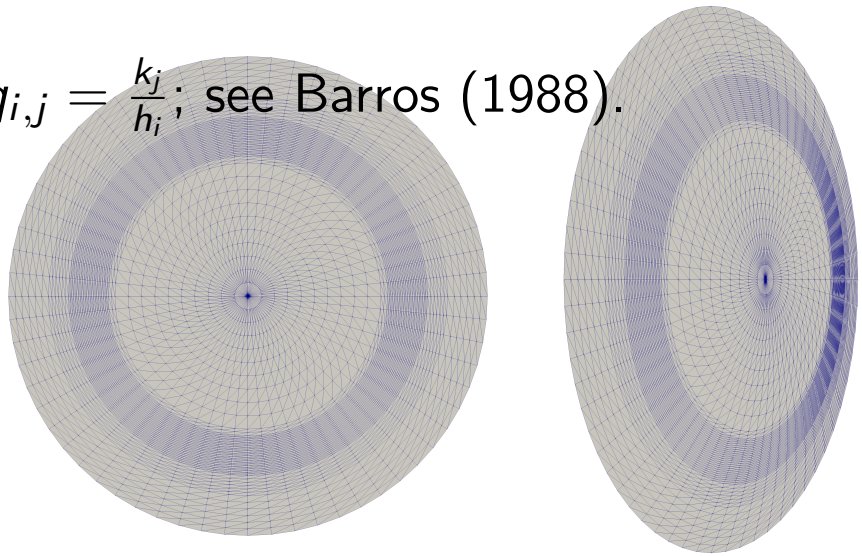

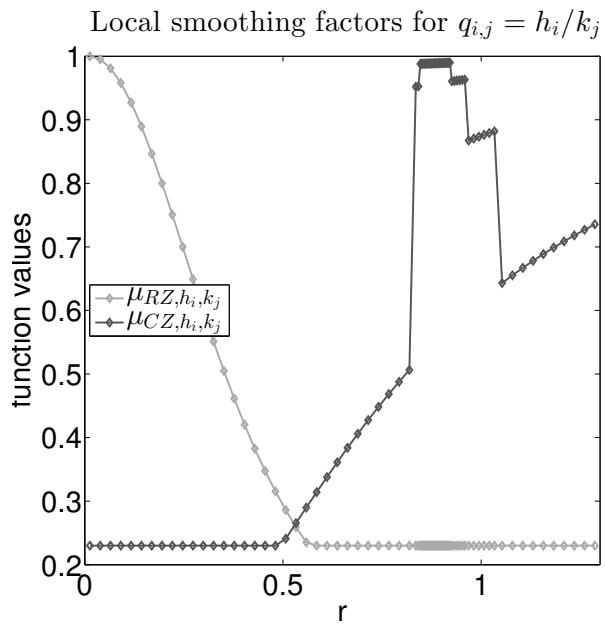

Parallel circle-radial smoothing based on local optimization

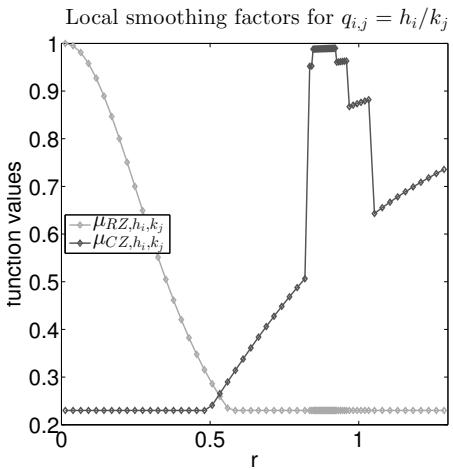

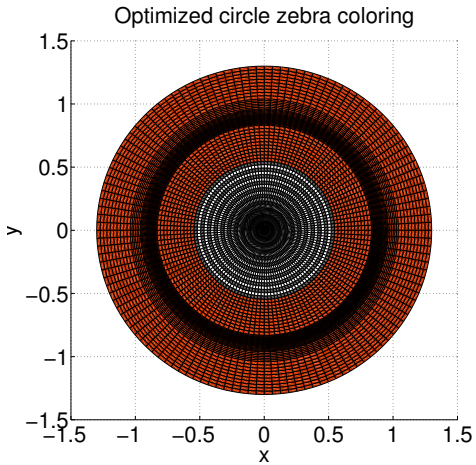

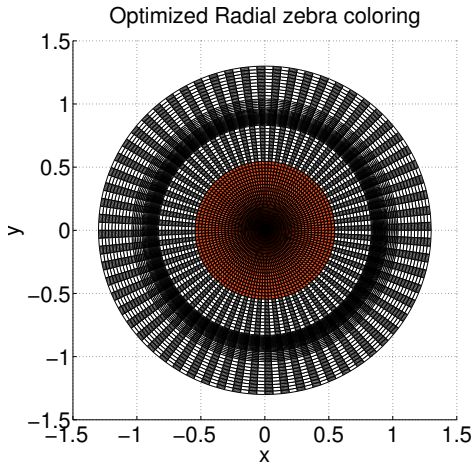

- circle smoothing around origin
- change to radial smoothing where curves intersect
- nonoverlapping decomposition
- circle and radial smoothing executed in parallel
  (red parts not smoothed by half-step of smoother)
- optimal complexity $\mathcal{O}(n)$

Numerical results: preliminaries

- all results on deformed geometry
  (if not stated otherwise)
- maximum number of iterations: 150
- relative residual reduction by a factor of 10^8
- mean residual reduction

$$\widehat{\rho} = \sqrt[\text{its}]{\frac{\|r_L^0\|_2}{\|r_L^{\text{its}}\|_2}}$$

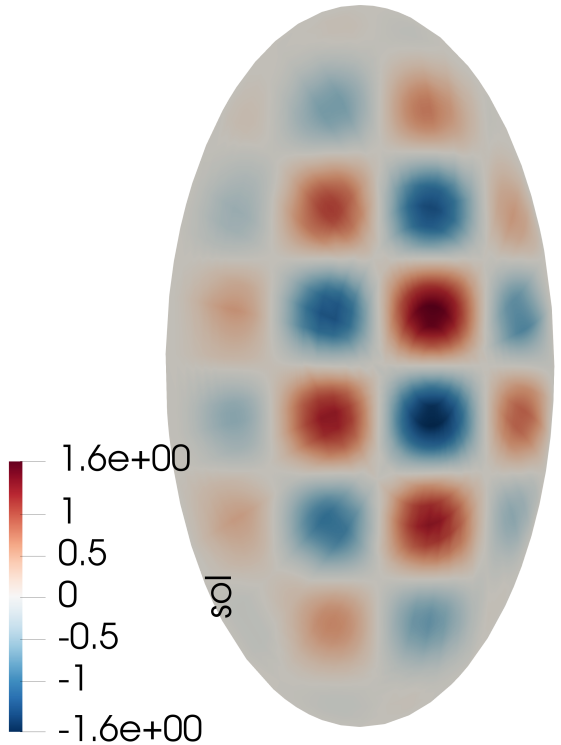

- nodal error comparison with manufactured exact solution

$$u(x,y) = (1.3^2 - r^2(x,y))\cos(2\pi x)\sin(2\pi y)$$

from Zoni/Güclü (2019).

Smoother comparison for MG without extrapolation (FD 9p)

	circle smoothing				*radial smoothing*			
$n_r \times n_\theta$	its	$\widehat{\rho}$	$\|err\|_{\ell_2}$	$\|err\|_\infty$	its	$\widehat{\rho}$	$\|err\|_{\ell_2}$	$\|err\|_\infty$
49×64	150	0.98	7.6e-02	1.5e-01	150	0.95	7.1e-02	1.5e-01
97×128	150	0.98	3.4e-02	1.4e-01	150	0.97	1.8e-02	4.1e-02
193×256	150	0.98	3.0e-02	1.4e-01	150	0.97	4.7e-03	1.5e-02
385×512	150	0.98	2.9e-02	1.4e-01	150	0.97	1.6e-03	1.5e-02

	optimized smoothing			
$n_r \times n_\theta$	its	$\widehat{\rho}$	$\|err\|_{\ell_2}$	$\|err\|_\infty$
49×64	46	0.67	7.1e-02	1.5e-01
97×128	45	0.66	1.8e-02	4.1e-02
193×256	44	0.66	4.5e-03	1.1e-02
385×512	44	0.65	1.1e-03	2.6e-03

Implicitly extrapolated MG for $r_1 \in \{1e-5, 1e-8\}$

with Dirichlet BC and *across the origin*, resp.: four different configurations !

$n_r \times n_\theta$	its	$\widehat{\rho}$	$\|err\|_{\ell_2}$	*ord.*	$\|err\|_\infty$	*ord.*	its	$\widehat{\rho}$	$\|err\|_{\ell_2}$	*ord.*	$\|err\|_\infty$	*ord.*
	FE P1 (nonstandard integ.)						*FD 9p*					
49×64	76	0.78	7.9e-03	-	3.0e-02	-	73	0.78	7.6e-03	-	2.6e-02	-
97×128	81	0.80	6.1e-04	3.69	4.3e-03	2.82	78	0.79	5.6e-04	3.76	2.9e-03	3.13
193×256	83	0.80	4.8e-05	3.67	4.5e-04	3.24	78	0.79	4.2e-05	3.72	3.6e-04	3.01
385×512	85	0.80	3.7e-06	3.71	4.5e-05*	3.35	79	0.79	3.2e-06	3.71	4.5e-05*	3.00

*: For the four different configurations, the values lie in [4.4e-05,4.5e-05]

Multigrid for the gyrokinetic Poisson equation

- introduction of curvilinear description leads to anisotropy
  $\rightarrow$ parallel circle-radial smoothing: optimal complexity and good smoothing
- ...artificial singularity
  $\rightarrow$ across the origin discretization as good as Dirichlet BC
- density profile and anistropic grid refinement
  $\rightarrow$ no additional difficulty for our multigrid solver
- still fast convergence for deformed geometry
- optimal complexity of one multigrid cycle
- implicit extrapolation raises convergence order up to 3.7 (3 in max norm)
- matrix-free FD numerically as valid as FE with nonstandard quadrature

Thank you for your attention!

- M. J. Kühn, C. Kruse, U. Rüde, *Energy-minimizing, symmetric finite differences for anisotropic meshes and energy functional extrapolation* (2020). Submitted. Preprint: `https://hal.archives-ouvertes.fr/hal-02941899`
- M. J. Kühn, C. Kruse, U. Rüde, *Implicitly extrapolated geometric multigrid on disk-like domains for the gyrokinetic Poisson equation from fusion plasma applications* (2020). Submitted. Preprint: `https://hal.archives-ouvertes.fr/hal-03003307`

The funding from the European Union's Horizon 2020 research and innovation programme under grant agreement no. 824158 is greatfully acknowledged.

DLR

Additional material

Discretization: Nonstandard FE integration

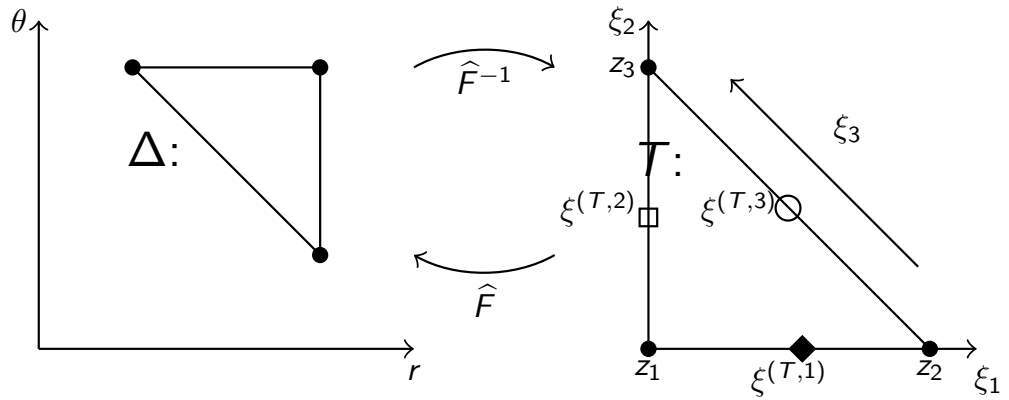

Figure: Mesh element Δ (left) and reference triangle T (right).
Directions $\xi_1 = e_1$, $\xi_2 = e_2$, and $\xi_3 = e_2 - e_1$.
Evaluation nodes $\xi^{(T,1)}$, $\xi^{(T,2)}$, and $\xi^{(T,3)}$ (right).

$$\int_T \left(b^{\xi_1\xi_1} \frac{\partial \widehat{\varphi}_{\widehat{\alpha}}}{\partial \xi_1} \frac{\partial \widehat{\varphi}_{\widehat{\beta}}}{\partial \xi_1} + b^{\xi_2\xi_2} \frac{\partial \widehat{\varphi}_{\widehat{\alpha}}}{\partial \xi_2} \frac{\partial \widehat{\varphi}_{\widehat{\beta}}}{\partial \xi_2} + b^{\xi_3\xi_3} \frac{\partial \widehat{\varphi}_{\widehat{\alpha}}}{\partial \xi_3} \frac{\partial \widehat{\varphi}_{\widehat{\beta}}}{\partial \xi_3} \right) \mathrm{d}(\xi_1, \xi_2)$$

$$\approx |T| \sum_{n=1}^{3} b^{\xi_n\xi_n} \left(\xi^{(T,n)}\right) \frac{\partial \widehat{\varphi}_{\widehat{\alpha}}}{\partial \xi_n} \left(\xi^{(T,n)}\right) \frac{\partial \widehat{\varphi}_{\widehat{\beta}}}{\partial \xi_n} \left(\xi^{(T,n)}\right)$$

Discretization: Matrix-free symmetric FD

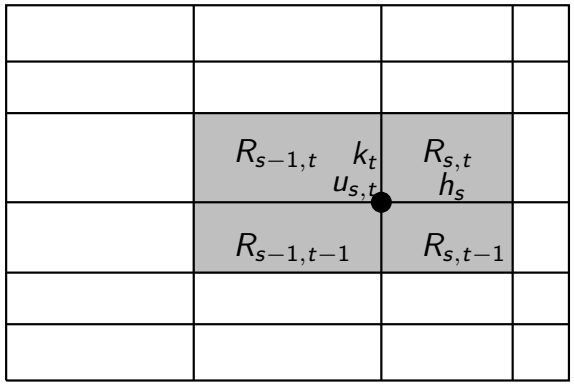

- Discretize energy functional

$$J^{\text{lhs}}_{R_{ij}}(u) := \int_{R_{ij}} \left(a^{rr}u_r^2 + a^{r\theta}u_r u_\theta + a^{\theta\theta}u_\theta^2\right) \mathrm{d}(r,\theta) =: \widetilde{J}^{\text{lhs}}_{R_{ij}}(u) + \mathcal{O}(h_i k_j)$$

  (use first order approximations and numerical integration)
- $I_{s,t} := \{(s,t),(s-1,t),(s,t-1),(s-1,t-1)\}$
- Critical point condition

$$\sum_{(i,j)\in I_{s,t}} \frac{\partial}{\partial u_{s,t}} \left(\widetilde{J}^{\text{lhs}}_{R_{ij}}(u) + \widetilde{J}^{\text{rhs}}_{R_{ij}}(u)\right) = 0$$

  yields the finite difference stencil.

On the optimization of the smoother parallelization (FD 5p and 9p)

Multigrid **without** extrapolation:

		Circular geometry		*Deformed geometry*	
$n_r \times n_\theta$	decomp	its	$\widehat{\rho}$	its	$\widehat{\rho}$
145×256	optim. circ.	8	0.09	19	0.36
	optim. circ.-4	9	0.11	19	0.36
	optim. circ.-8	11	0.16	22	0.43
	optim. circ.+4	15	0.27	30	0.53
	optim. circ.+8	26	0.48	48	0.68

Implicitly extrapolated MG for $r_1 = 1e-2$ on circular geometry

$n_r \times n_\theta$	its	$\widehat{\rho}$	$\|err\|_{\ell_2}$	*ord.*	$\|err\|_\infty$	*ord.*	its	$\widehat{\rho}$	$\|err\|_{\ell_2}$	*ord.*	$\|err\|_\infty$	*ord.*
	FE P1 (nonstandard integ.)						*FD 9p*					
Dirichlet boundary conditions on innermost circle												
49×64	36	0.60	3.6e-03	-	1.7e-02	-	36	0.60	3.6e-03	-	1.7e-02	-
97×128	38	0.61	2.4e-04	3.92	1.5e-03	3.46	38	0.61	2.4e-04	3.91	1.5e-03	3.45
193×256	38	0.61	1.7e-05	3.79	1.5e-04	3.28	38	0.61	1.7e-05	3.79	1.6e-04	3.27
385×512	36	0.60	1.3e-06	3.74	1.7e-05	3.16	36	0.60	1.3e-06	3.75	1.8e-05	3.16
Discretization across the origin												
49×64	37	0.60	3.6e-03	-	1.6e-02	-	36	0.60	4.5e-03	-	1.9e-02	-
97×128	38	0.61	2.3e-04	3.94	1.5e-03	3.46	38	0.61	2.3e-03	0.99	2.8e-02	-0.56
193×256	39	0.62	1.8e-05	3.71	1.5e-04	3.27	39	0.62	2.0e-03	0.21	3.3e-02	-0.22
385×512	39	0.62	5.6e-06	1.64	8.9e-05	0.81	39	0.62	1.7e-03	0.21	3.5e-02	-0.08

Implicitly extrapolated MG for $r_1 \in \{1e-5, 1e-8\}$ on circular geometry

with Dirichlet BC and *across the origin*, resp.: four different configurations !

$n_r \times n_\theta$	its	$\widehat{\rho}$	$\|err\|_{\ell_2}$	*ord.*	$\|err\|_\infty$	*ord.*	its	$\widehat{\rho}$	$\|err\|_{\ell_2}$	*ord.*	$\|err\|_\infty$	*ord.*
49×64	37[*1]	0.61[*2]	3.6e-03	-	1.6e-02	-	37[*1]	0.61[*2]	3.6e-03	-	1.6e-02	-
97×128	38	0.61	2.4e-04	3.92	1.5e-03	3.45	38	0.61	2.4e-04	3.91	1.5e-03	3.44
193×256	39	0.62	1.8e-05	3.76	1.8e-04	3.08	39	0.62	1.8e-05	3.75	1.8e-04	3.09
385×512	39	0.62	1.4e-06	3.64	2.2e-05	3.00	39	0.62	1.4e-06	3.65	2.2e-05	3.00

[*1]: For the four different configurations, the values lie in $\{36, 37\}$

[*2]: For the four different configurations, the values lie in $\{0.60, 0.61\}$

Multigrid without extrapolation for $r_1 \in \{1e-5, 1e-8\}$

with Dirichlet BC and *across the origin*, resp.: four different configurations !

$n_r \times n_\theta$	its	$\widehat{\rho}$	$\|err\|_{\ell_2}$	*ord.*	$\|err\|_\infty$	*ord.*	its	$\widehat{\rho}$	$\|err\|_{\ell_2}$	*ord.*	$\|err\|_\infty$	*ord.*
Circular geometry												
	FE P1 (nonstandard integ.)						*FD 5p*					
49×64	13	0.23	5.1e-02	-	9.6e-02	-	13	0.23	5.1e-02	-	9.6e-02	-
97×128	13	0.23	1.3e-02	2.01	2.4e-02	2.00	13	0.23	1.3e-02	2.00	2.4e-02	2.01
193×256	13	0.22	3.2e-03	2.00	6.0e-03	2.00	13	0.22	3.2e-03	2.00	6.0e-03	2.00
385×512	13	0.22	8.0e-04	2.00	1.5e-03	2.00	13	0.22	8.0e-04	2.00	1.5e-03	2.00
Deformed geometry												
	FE P1 (nonstandard integ.)						*FD 9p*					
49×64	46	0.67	7.2e-02	-	1.6e-01	-	46	0.67	7.1e-02	-	1.5e-01	-
97×128	45	0.66	1.8e-02	1.98	4.7e-02	1.79	45	0.66	1.8e-02	1.98	4.1e-02	1.86
193×256	44	0.66	4.6e-03	1.99	1.2e-02	1.93	44	0.66	4.5e-03	1.99	1.1e-02	1.95
385×512	44	0.65	1.2e-03	2.00	3.1e-03	1.98	44	0.65	1.1e-03	2.00	2.6e-03	1.99

Implicitly extrapolated MG for $r_1 = 1e-2$

$n_r \times n_\theta$	its	$\widehat{\rho}$	$\|err\|_{\ell_2}$	*ord.*	$\|err\|_\infty$	*ord.*	its	$\widehat{\rho}$	$\|err\|_{\ell_2}$	*ord.*	$\|err\|_\infty$	*ord.*
	FE P1 (nonstandard integ.)						*FD 9p*					
Dirichlet boundary conditions on innermost circle												
49×64	77	0.79	7.9e-03	-	3.0e-02	-	75	0.78	7.5e-03	-	2.6e-02	-
97×128	81	0.80	6.1e-04	3.68	4.3e-03	2.81	79	0.79	5.6e-04	3.75	3.0e-03	3.12
193×256	81	0.80	4.8e-05	3.68	4.5e-04	3.25	77	0.79	4.2e-05	3.73	3.4e-04	3.12
385×512	77	0.79	3.5e-06	3.76	4.0e-05	3.49	73	0.78	3.1e-06	3.77	4.0e-05	3.10
Discretization across the origin												
49×64	77	0.79	8.1e-03	-	3.0e-02	-	75	0.78	8.6e-03	-	2.5e-02	-
97×128	82	0.80	1.7e-03	2.23	1.6e-02	0.92	80	0.79	3.3e-03	1.40	3.7e-02	-0.58
193×256	84	0.80	1.4e-03	0.31	1.9e-02	-0.30	80	0.79	2.8e-03	0.23	4.5e-02	-0.27
385×512	85	0.80	1.2e-03	0.21	2.1e-02	-0.14	80	0.79	2.5e-03	0.19	4.9e-02	-0.12